4-71

HIGHLY TUNABLE AND EFFICIENT DIODE PUMPED OPERATION OF Tm^{3+} DOPED FIBRE LASERS

Indexing terms: Lasers and laser applications, Semiconductor lasers, Doping

The characteristics of a Tm^{3+} doped fibre laser pumped by a laser diode are reported. Operating at a wavelength of 1·94 μm, the laser had a threshold of 4·4 mW, a launched power slope efficiency of 17% and 1 mW output power. Measurements on the tuning range of Tm^{3+} are presented and lasing is found to be possible from 1·65–2·0 μm, the specific range depending on the fibre type. The largest range for a single laser was 300 nm.

Lasers operating around 2 μm are of interest for medical applications for optical sensors and as spectroscopic sources. The rare earth ion Tm^{3+} has a suitable energy level scheme for these wavelengths and should be broadly tunable in glass. The $^3H_4 \rightarrow {}^3H_6$ transition is quasi three level, so early demonstrations of lasing were made at low temperatures.[1]

The guided wave nature of fibre lasers provides a high pump intensity in the fibre core for modest input pump powers. This intensity is maintained over a long interaction length. As a result it is possible to bleach three level transitions and obtain lasing with relative ease, as has been demonstrated with Er^{3+}.[2,3] The $^3H_4 \rightarrow {}^3H_6$ transition of Tm^{3+} can be easily operated at room temperature and recent reports[4–6] have indicated that diode pumped operation should be possible.

Tm^{3+} fibre lasers pumped through the $^3F_4$ band (785 nm) have required launched pump powers in excess of 30 mW to reach threshold. This has been partly because of pumping into the edge of the absorption band and partly because of the reduced $^3H_4$ level lifetimes of fibres used in previous work. Two new fibres were made by the solution doping technique.[7] One comprised a GeO_2–SiO_2 core with a dopant concentration of 50 ppm, $NA = 0{\cdot}2$ and a cutoff of 1·1 μm. The other was an Al_2O_3–SiO_2 glass, had a dopant concentration of 200 ppm, $NA = 0{\cdot}15$ and a cutoff of 1·1 μm. In the GeO_2–SiO_2 host the $^3H_4$ lifetime was ~300 μs, and in Al_2O_3–SiO_2 ~ 500 μs. All experiments were conducted at room temperature.

A double butter cavity was used for the diode pumped experiments. The pump laser diode operated at 786 nm and 15 mW of pump power could be launched into the fibre. Using 0·45 m of the Al_2O_3–SiO_2 fibre lasing was obtained at a wavelength of 1·94 μm. Several different output couplers were used, $R = 90\%$, 95% and >99·5%. (Threshold was unobtainable for $R = 80\%$). Fig. 1 shows the lasing characteristic obtained with the $R = 90\%$ coupler. The launched power was calculated from the diode output power by measuring the launch efficiency (at low drive currents). The launched pump power required to reach threshold was just 4·4 mW. The turn over in the laser characteristic at high pump powers is an artifact caused by the change in launch efficiency of the diode when driven hard—it is not believed to be intrinsic to the fibre laser. Bearing this in mind the slope efficiency (with respect to launched pump power) is 17%, the quantum efficiency is estimated to be 1·0.

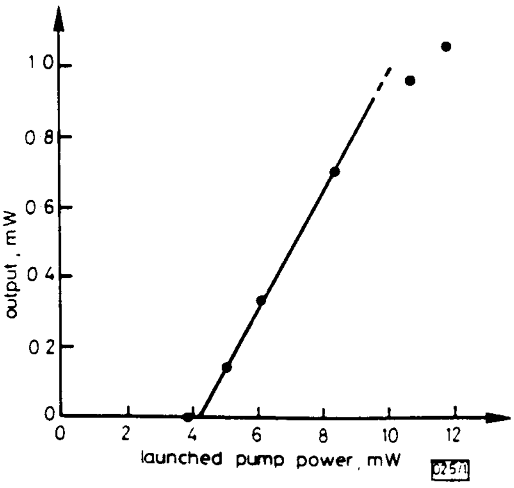

Fig. 1 *Diode pumped lasing characteristic*

Diode pumped operation was also possible with the GeO_2–SiO_2 fibre, lasing occurred at ~1·84 μm for a fibre length of 5 m. The operating wavelengths for these two lasers depend on both the length of fibre and the spectral characteristic of the output coupler. We believe the difference in operating wavelength to be largely intrinsic to the two glass hosts.

The laser tuning ranges for the two fibre types were measured using a laser with a grating (ruled, and blazed for 1 μm) as the output coupler.[2] An Ar^+ pumped $Ti^{3+}:Al_2O_3$ laser was used as the pump source at 788 nm. To overcome the loss of the tuning cavity more gain was required. This was achieved by using longer lengths of fibre and higher pump powers. As a result the thresholds for the tuned laser are significantly higher than those for the double butted cavity. The Al_2O_3–SiO_2 fibre had sufficient gain to lase at 1·85 μm of the Fresnel reflection of the fibre end. We estimate the gain at 1·85 μm to be ~0·2 dB/mW.

Fig. 2 shows the measured tuning range for the two fibres. Both are very broad, the Al_2O_3–SiO_2 being almost 300 nm.

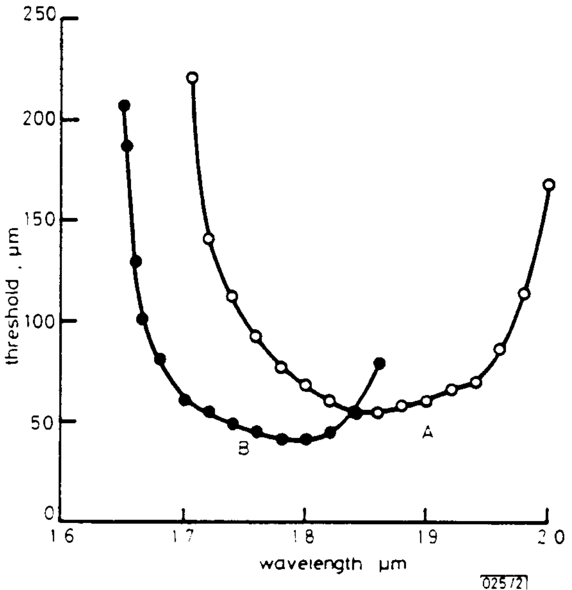

Fig. 2 *Tuning ranges*

A: Al_2O_3–SiO_2 fibre
B: GeO_2–SiO_2 fibre

The lower wavelength limits of interest in the GeO_2–SiO_2 curve. Lasing was possible down to 1·65 μm, and is thus of interest for methane sensing where a C–H bond overtone is centred at 1·668 μm. The considerable difference in operating ranges of the two fibre types suggests that other hosts might extend the tuning range still further.

In conclusion we have demonstrated efficient laser diode pumped operation of a Tm^{3+} fibre laser. The Tm^{3+} fibre laser may now be considered a practical source in the 1·65–2·0 μm wavelength range. We have also shown the large tuning range that is possible and indicated the considerable effect of the glass host.

Acknowledgments: This work was supported in part by the Amoco Technology Company. The authors would like to acknowledge the assistance of J. Lincoln of the Physics department at Southampton University in this work.

W. L. BARNES
J. E. TOWNSEND

Optical Fibre Group
The University
Southampton SO9 5NH, United Kingdom

26th March 1990

References

1 GANDY, H. W., GINTHER, R. J., and WELLER, J. F.: 'Stimulated emission of Tm^{3+} radiation in silicate glass', *J. Appl. Phys.*, 1967, **38**, pp. 3030–3031

2 MEARS, R. J., REEKIE, L., POOLE, S. B., and PAYNE, D. N.: 'Low-threshold tunable CW and Q-switched fibre laser operating at 1·55 μm', *Electron. Lett.*, 1986, **22**, pp. 159–160

3 BARNES, W. L., MORKEL, P. R., REEKIE, L., and PAYNE, D. N.: 'High quantum efficiency Er^{3+} fibre lasers pumped at 980 nm', *Opt. Lett.*, 1989, **14**, pp. 1002–1004

4 HANNA, D. C., JAUNCEY, I. M., PERCIVAL, R. M., PERRY, I. R., SMART, R. G., SUNI, P. J., TOWNSEND, J. E., and TROPPER, A. C.: 'Continuos wave oscillation of a monomode thulium-doped fibre laser', *Electron. Lett.*, 1988, **24**, pp. 1222–1223

5 HANNA, D. C., PERCIVAL, R. M., SMART, R. G., and TROPPER, A. C.: 'Efficient and tunable operation of a Tm-doped fibre laser', to be published in *Optics Communications*

6 FAN, T. Y., and BYER, R. L.: 'Diode laser pumped solid state lasers', *IEEE J. Quantum Electron.*, 1988, **QE-24**, pp. 895–912

7 TOWNSEND, J. E., POOLE, S. B., and PAYNE, D. N.: 'Solution-doping technique for fabrication of rare-earth-doped optical fibres', *Electron. Lett.*, 1987, **23**, pp. 329–331

MEASUREMENTS OF PULSE PROPAGATION ON UNTERMINATED LOSSY MICROSTRIPS WITH SMALL DIMENSIONS

Indexing terms: Data transmission, Microstrip, Large scale integration

An unterminated small microstrip (2·5 μm thick and 20 μm wide) up to a length of $\sim$20 cm, can adequately transmit digital signals, with 50 MHz frequency and 2 ns rise time, when driven and received by the recent advanced CMOS chips. Owing to the short interconnection length offered by these high-density, unterminated small microstrips, small CMOS drivers with fewer cascade stages can be used. A high performance, high integration VLSI machine built on a small substrate can therefore be achieved.

Lossy microstrips with small dimensions on either ceramics or silicon substrates have been proposed to interconnect VLSI chips.[1,2] In the past few years, there has been an increase in effort in the electronics industry to develop high density interconnection technology based on these small microstrips.[3] The line resistance of small microstrips can be used to dampen the reflection so an unterminated interconnection scheme can be achieved. The unterminated, high density interconnection is desirable for high speed VLSI chips (with a frequency of $\sim$100 MHz and a rise time of $\sim$1 ns). The aim of this letter is to demonstrate the feasibility of this unterminated interconnection scheme by the direct measurements of pulse propagation on these small microstrips.

Fig. 1 shows the importance of these small microstrips in interconnecting VLSI chips. The frequency of electronic machines is related to the interconnection length as in the following arguments: For a given machine frequency, f, the rise time, t_r, on the left scale of Fig. 1, can be derived using an assumed machine architecture with a 1 : 16 ratio between the rise time and the repetitive pulse duration. The main frequency component in the rise time region is $f_r = 1/2t_r$. Fig. 1 is obtained by considering the standing waves, $f_r = v/\lambda_r = v/2l$, and $f_r = 8f$, where $v = c/\sqrt{(\varepsilon)}$ is the velocity, $\varepsilon = 3·5$ is the dielectric constant, λ_r is the wavelength corresponding to f_r, and l is the length of the microstrips. For $l > \lambda_r/2$, the microstrips behave as transmission lines, and termination is required. For $l \ll \lambda_r/2$, they can be treated as a lumped-element circuit and no termination is required. In the region in which $\lambda_r/32 < l < \lambda_r/2$, the lossy transmission lines can be used without termination by using the line resistance to dampen the reflection. The most widely used VLSI chips at the present time and in the near future are at frequencies of between 10 and 100 MHz and have rise times of between 0·6 and 6 ns. Therefore most of the complicated VLSI systems can be built on the multichip package based on the unterminated small microstrips, which are fabricated on silicon or ceramics substrates. The whole package dimension will be smaller than 10 cm.

The setup for measuring the unterminated microstrips is shown in Fig. 2. The small microstrips used in experiments are fabricated on silicon substrates.[4] The conductor consists of 2·5 μm of copper with a 0·3 μm nickel cap, and is embedded in the polyimide dielectrics ($h_1 = h_2 = 10\,\mu$m) as shown in Fig. 3. The four-stage cascade CMOS drivers are used to drive the microstrips and to receive the output pulses. This CMOS driver was originally designed for use in the conventional single chip package and printing-wiring boards. The circuit design, as shown in Fig. 4, aims to drive a capacitive load of 50 pF, and is optimised for the minimum stage-up delay. The

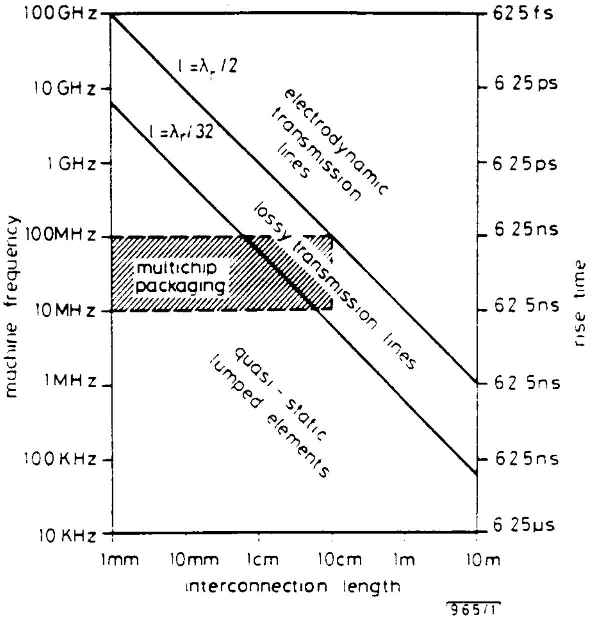

Fig. 1 *Machine frequency and rise time against interconnection length*

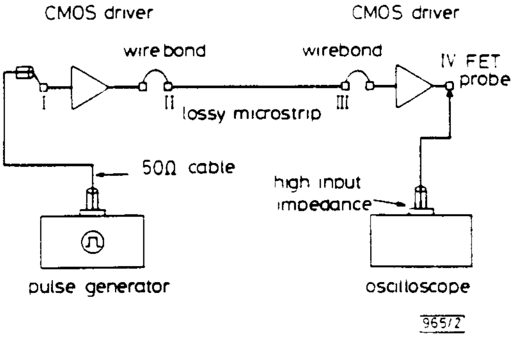

Fig. 2 *Setup for measuring unterminated microstrips*

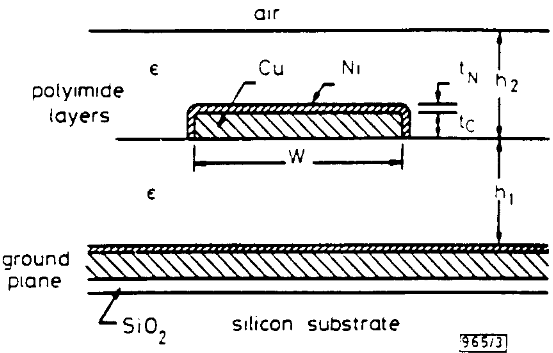

Fig. 3 *Cross-section of microstrips*

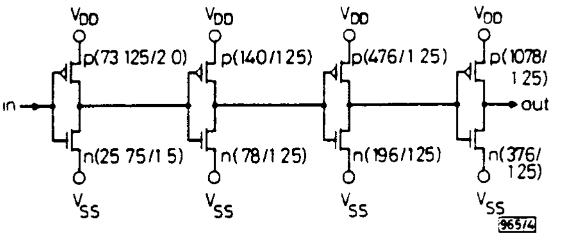

Fig. 4 *Circuit of four-stage cascade CMOS driver*